# Amplified spontaneous emission and optical gain measurements from pyrromethene 567 – doped polymer waveguides and quasi-waveguides

**A. Costela [1,*], O. García [2], L. Cerdán [1], I. García-Moreno [1], and R. Sastre [1]**

[1] Instituto de Química Física "Rocasolano", C.S.I.C., Serrano 119, 28006 Madrid, Spain
[2] Instituto de Ciencia y Tecnología de Polímeros, C.S.I.C., Juan de la Cierva 3, 28006 Madrid, Spain
[*] *Corresponding author:* acostela@iqfr.csic.es

**Abstract:** Amplified spontaneous emission from planar waveguides and quasi-waveguides based on Pyrromethene 567-doped poly(methyl methacrylate) thin films deposited onto quartz and glass substrates is investigated. Films with different thickness were prepared and pumped optically at 532 nm with pulses of up to 8 MW/cm$^2$. Pump thresholds for the onset of ASE emission, optical gains and losses were assessed. Net gain coefficients were estimated by fitting the data provided by variable stripe length measurements with a theoretical expression which takes into account saturation. In this way, net gain coefficients of up to 56 ± 9 cm$^{-1}$ at a pump intensity of 5.3 MW/cm$^2$ for quasi-waveguides and up to 20.6 ± 2.7 cm$^{-1}$ at a pump intensity of 3.4 MW/cm$^2$ for waveguides, were obtained. Loss coefficients in the waveguides were estimated to be 3.8 ± 0.4 cm$^{-1}$ and 6.1 ± 1.3 cm$^{-1}$ for 15 μm and 5 μm thick films, respectively. The results obtained seem to indicate a stronger self-mode-restriction capability in the quasi-waveguides than in conventional total internal-reflection waveguides.



**OCIS codes:** (140.2050) Dye lasers; (140.3380) laser materials; (230.7390) Waveguides, planar; (230.310) Thin films; (250.2080) Polymer active devices; (250.5460) Polymer waveguides.

## References and links

1. A. Costela, I. García-Moreno, and R. Sastre, "Materials for solid-state dye lasers," in *Handbook of Advanced Electronic and Photonic Materials and Devices*, H.S. Nalwa, ed. (Academic, San Diego, Ca., 2001), vol. 7, Chap. 4, p.161.
2. A. Costela, I. García-Moreno, and R. Sastre, "Polymeric solid-state dye lasers: recent developments," Phys. Chem. Chem. Phys. **5**, 4745-4763 (2003).
3. K. P. Kretsch, C. Belton, S. Lipson, W. J. Blau, F. Z. Henari, H. Rost, S. Pfeiffer, A. Teuschel, H. Tillmann, and H.-H. Hörhold, "Amplified spontaneous emission and optical gain spectra from stilbenoid and phenylene detrivative model compounds," J. Appl. Phys. **86**, 6155-6159 (1999).
4. H. Manaa and S. M. Al-Alawi, "Optical gain measurements in polymethyl methacrylate plastic doped with perylimide dyes," J. Lumin. **94-95**, 55-58 (2001).
5. M. C. Castex, C. Olivero, A. Fischer, S. Mousel, J. Michelon, D. Adês, and A. Siove, "Polycarbazoles microcavities: towards plastic blue lasers," Appl. Surf. Sci. **197-198**, 822-825 (2002).
6. Y. Kawabe, L. Wang, T. Nakamura, and N. Ogata, "Thin-film lasers based on dye-deoxyribonucleic acid-lipid complexes," Appl. Phys. Lett. **81**, 1372-1374 (2002).
7. A. K. Sheridan, A. R. Buckley, A. M. Fox, A. Bacher, D. D. C. Bradley, and I. D. W. Samuel, "Efficient energy-transfer in organic thin films-implications for organic laser," J. Appl. Phys. **92**, 6367-6371 (2002).
8. S.-S. Yap, W.-O. Siew, T.-Y. Tou, and S.-W. Ng, "Red-green-blue laser emission from dye-doped poly(vinyl alcohol) films," Appl. Opt. **41**, 1725-1728 (2002).
9. Y. Oki, S. Miyamoto, M. Maeda, and N. J. Vasa, "Multiwavelength distributed-feedback dye laser array and its application to spectroscopy," Opt. Lett. **27**, 1220-1222 (2002).
10. Y. Oki, T. Yoshiura, Y. Chisaki, and M. Maeda, "Fabrication of a distributed-feedback dye laser with a grating structure in its plastic waveguide," Appl. Opt. **41**, 5030-5035 (2002).
11. Y. Oki, S. Miyamoto, M. Tanaka, D. Zuo, and M. Maeda, "Long lifetime and high repetition rate operation from distributed feedback plastic waveguided dye lasers," Opt. Commun. **214,** 277-383 (2002).

#93332 - $15.00 USD Received 29 Feb 2008; revised 7 Apr 2008; accepted 15 Apr 2008; published 1 May 2008

12. Y. Oki, M. Tanaka, Y. Ogawa, H. Watanabe, and M. Maeda, "Development of Quasi-End-Fired Waveguide Plastic Dye Laser," IEEE J. Quantum Electron. **42,** 389-396 (2006).
13. N. Tsutsumi, T. Kawahira, and W. Sakai, "Amplified spontaneous emission and distributed feedback lasing from a conjugated compound in various polymer matrices,"Appl. Phys. Lett. **83**, 2533-2535 (2003).
14. N. Tsutsumi, A. Fujihara, and D. Hayashi, "Tunable distributed feedback lasing with a threshold in the nanojoule range in an organic guest-host polymeric waveguide," Appl. Opt. **45,** 5748-5751 (2006).
15. M. A. Reilly, C. Marinelli, C. N. Morgan, R. V. Penty, I. H. White, M. Ramon, M. Ariu, R. Xia, and D. D. C. Bradley, "Rib waveguide dye-doped polymer amplifier with up to 26 dB optical gain at 625 nm," Appl. Phys. Lett. **85,** 5137-5139 (2004).
16. M. A. Reilly, B. Coleman, E. Y. B. Pun, R. V. Penty, I. H. White, M. Ramon, R. Xia, and D. D. C. Bradley, "Optical gain at 650 nm from a polymer waveguide with dye-doped cladding," Appl. Phys. Lett. **87,** (2005) 231116 (2005).
17. W. Lu, B. Zhong, and D. Ma, "Amplified spontaneous emission and gain from optically pumped films of dye-doped polymers," Appl. Opt. **43**, 5074-5078 (2004).
18. D. Zhang and D. Ma, "Improved amplified spontaneous emission by doping of green fluorescent dye C545T in red fluorescent dye DCJTB:PS polymer films," Appl. Opt. **46**, 2996-3000 (2007).
19. E. V. Calzado, J. M. Villalvilla, P. G. Boj, J. A. Quintana, and M. A. Díaz García, "Tuneability of amplified spontaneous emission through control of the thickness in organic-based waveguides," J. Appl. Phys. **7**, 093103 (2005).
20. E. V. Calzado, J. M. Villalvilla, P. G. Boj, J. A. Quintana, R. Gómez, J. L. Segura, and M. A. Díaz García, "Effect of structural Modifications in the Spectral and Laser properties of Perylendiimide Derivatives," J. Phys Chem. **111**, 13595-13605 (2007).
21. E. V. Calzado, J. M. Villalvilla, P. G. Boj, J. A. Quintana, R. Gómez, J. L. Segura, and M. A. Díaz García, "Amplified spontaneous emission in polymer films doped with a perylenediimide derivative," Appl. Opt. **46,** 3836-3842 (2007).
22. R. Kumar, A. P. Singh, A. Kapoor, and K. N. Tripathi, "Effect of dye doping in poly(vinyl alcohol) waveguides," J. Mod. Opt. **10**, 1471-1483 (2005).
23. K. Sakai, T. Tsuzuki, Y. Itoh, M. Ichikawa, and Y. Taniguchi, "Using proton-transfer dyes for organic laser diodes," Appl. Phys. Lett. **86**, 081103 (2005).
24. K. Geetha, M. Rajesh, V. P. N. Nampoori, C. P. G. Vallabhan, and P. Radhakrishnan, "Laser emission from transversely pumped dye-doped free-standimg polymer film," J. Opt. A: Pure Appl. Opt. **8**, 189-193 (2006).
25. G. Jordan, M. Flämmich, M. Rüther, T. Kobayashi, and W. J. Blau, "Light amplification at 501 nm and large nanosecond optical gain in organic dye-doped polymeric waveguides," Appl. Phys. Lett. **88**, 161114 (2006).
26. D. Pisignano, E. Mele, L. Persano, A. Athanassiou, C. Fotakis, and R. Cingolani, "Optical gain from the Open Form of a Photochromic Molecule in the Solid State," J. Phys. Chem. B **110**, 4506-4509 (2006).
27. M. Kawasaki and S. Mine, "Novel lasing Action in Dye-Doped Polymer Films Coated on large Pseudotabular Ag Islands," J. Phys. Chem. B **110**, 15052-15054 (2006).
28. H. Goudket, T. H. Nhung, B. Ea-Kim, G. Roger, and M. Canva, "Importance of dye host on absorption, propagation losses, and amplified spontaneous emission for dye-doped polymer thin films," Appl. Opt. **45**, 7736-7741 (2006).
29. Z. Yu, W. Li, J. A. Hagen, Y. Zhou, D. Klotzkin, J. G. Grote, and A.J. Steckl, "Photoluminescence and lasing from deoxyribonucleic acid (DNA) thin films doped with sulforhodamine," Appl. Opt. **46**, 1507-1513 (2007).
30. A. Büttner and U. D. Zeitner, "Experimental realization of Monolithic Diffractive Broad-Area polymeric Waveguide Dye Lasers," IEEE J. Quantum Electron. **43,** 545-551 (2007).
31. P. Yang, G. Wirnsberger, H. C. Huang, S. R. Cordero, M. D. McGehee, B. Scott, T. Deng, G. M. Whitesides, B. F. Chmelka, S. K. Buratto, and G. D. Stucky, "Mirrorless Lasing from Mesostructured Waveguides Patterned by Soft Lithography," Science **287**, 465-467 (2000).
32. X. Zhu and D. Lo, "Sol-gel glass distributed-feedback waveguide laser," Appl. Phys. Lett. **80,** 917-919 (2002).
33. D. Lo, L. Shi, J. Wang, G.-X. Zhang, and X. Zhu, "Zirconia and zirconia-organically modified silicate distributed feedback waveguide lasers tunable in the visible," Appl. Phys. Lett. **81**, 2707-2709 (2002).
34. J. Wang, G.-X. Zhang, L. Shi, D. Lo,and X. Zhu, "Tunable multiwavelength distributed-feedback zirconia waveguide lasers," Opt. Lett. **28**, 90-92(2003).
35. D. Lo, C. Ye, and J. Wang, "Distributed feedback laser action by polarization modulation," Appl. Phys. B **76,** 649-653(2003).
36. C. J. Oton, D. Navarro-Urrios, N. E. Capuj, M. Ghulinyan, L. Pavesi, S. González-Pérez, F. Lahoz, and I. R. Martin, "Optical gain in dye-impregnated oxidized porous silicon waveguides," Appl. Phys. Lett. **89**, 011107 (2006).
37. X. Peng, L. Liu, J. Wu, Y. Li, Z. Hou, L. Xu, W. Wang, F. Li, and M. Ye, "Wide-range amplified spontaneous emission wavelength tuning in a solid-state dye waveguide," Opt. Lett. **25,** 314-316 (2000).
38. M. Casalboni, F. De Matteis, V. Merlo, P. Prosposito, R. Russo, and S. Schutzmann, "1.3 μm light amplification in dye-doped Irbid sol-gel channel waveguides," Appl. Phys. Lett., **83**, 416-418 (2003).

#93332 - $15.00 USD Received 29 Feb 2008; revised 7 Apr 2008; accepted 15 Apr 2008; published 1 May 2008

39. T. Saraidarov, R. Reisfeld, M. Kazes, and U. Banin, "Blue laser dye spectroscopic properties in sol-gel inorganic-organic hybrid films," Opt. Lett. **31,** 356-358 (2006).
40. T. G. Pavlopoulos, "Scaling of dye lasers with improved laser dyes," Prog. Quantum Electron. **26,** 193-224 (2002).
41. D. B. Hall and C. Yeh, "Leaky waves in a heteroepitaxial film," J. Appl. Phys. **44,** 2271-2274 (1973).
42. T.-N. Ding and E. Garmire, "Measuring refractive index and thickness of thin films: a new technique," Appl. Opt. **22**, 3177-3181 (1983).
43. K. Sasaki, T. Fukao, T. Saito, and O. Hamano, "Thin-film waveguide evanescent dye laser and its gain measurement," J. Appl. Phys. **51**, 3090-3092 (1980).
44. V. M. Arutuyan, G. P. Djotyan, A. V. Karmenyan, T. E. Melicksetyan, and E. M. Sarkissyan, "Thin-film narrowband tunable dye laser," Opt. Commun. **36,** 227-228 (1981).
45. D. Shamrakov and R. Reisfeld, "Superradiant film laser operation in red perylimide dye doped silica-polymethylmethacrylate," Chem. Phys. Lett. **213,** 47-53 (1993).
46. G. S. He, C. F. Zhao, C.-K. Park, P. N. Prasad, and R. Burzynski, "Dye film leaky waveguide laser," Opt. Commun. **111,** 82-85 (1994).
47. C. Lowe, *Surface Coatings Technology* (John Wiley&Sons, London, 1997), vol. 5, Chap. VI, p.60-62.
48. M. D. McGehee, R. Gupta, S. Veenstra, E. K. Miller, M. A. Díaz-García, and A. J. Heeger, "Amplified spontaneous emission from photopumped films of a conjugated polymer," Phys. Rev. B **58,** 7035-7039 (1998).
49. L. W. Casperson and A. Yariv, "Spectral narrowing in High-Gain Lasers," IEEE J. Quantum Electron. **QE-8**, 80-85 (1972).
50. A. Penzkofer, W. Holzer, H. Tillmann, and H.-H. Hörhold, "Leaky-mode emission of luminescent thin films on transparent substrates," Opt. Commun. **229**, 279-290 (2004).

## 1. Introduction

The development of tunable solid-state dye lasers, in which an organic dye is incorporated into a suitable solid matrix, is an area of active research [1,2]. While retaining the versatility of liquid dye lasers, these solid-state systems present a low-cost gain medium and are compact and easy to operate and maintain. On the other hand, active and passive waveguides are key components in a variety of photonic applications. Thus, the development of dye-doped thin films or waveguides, making use of the processing flexibility of these materials and combining the tunability and high efficiency of laser dyes with the high power density that can be easily achieved in waveguide structures, makes devices based on dye-doped waveguides very attractive and promising for optoelectronic applications.

Over the last years, amplified spontaneous emission (ASE) and lasing action have been achieved from organic [3-30], inorganic [31-36], and organic-inorganic [33,37-39] hybrid thin films and planar waveguides. A large amount of these studies have been carried out with dyes of the rhodamine family, mainly with the well known Rhodamine 6G (Rh6G) dye, and their properties as gain medium in thin films and waveguides have been thoroughly assessed [8-12,14-16,31-35]. Over the last decade, laser dyes of the pyrromethene family (4,4-difluor-3a,4a-diaza-4-boro-*s*-indacene dyes, also known as dipyrromethene.$BF_2$ (PM) dyes), with emission covering a spectral range wider than that of rhodamines, have become standard laser dyes for emission in the green-yellow to red regions of the spectrum because of their high efficiency and photostability in both liquid and solid gain media [1,40]. In spite of this, no reports on the optical gain properties of PM dyes in waveguides have appeared, apart from a few studies dealing with the importance of dye host on absorption, losses and ASE emission of Pyrromethene 597-doped polymer thin films [28], or with some characteristics of the laser output from Pyrromethene 567-doped plastic waveguides with distributed feedback structures [11].

In this paper, we present a systematic study on the properties of the ASE emission from thin films of poly(methyl methacrylate) (PMMA) doped with dye Pyrromethene 567 (PM567). Pump thresholds for the onset of ASE emission, gain coefficients and losses are determined for thin films of different thicknesses deposited onto quartz and glass substrates. For proper waveguiding operation the refractive index of the dye-doped polymer film has to be higher than that of the substrate. This condition is fulfilled when the PMMA-based films are deposited onto quartz slabs. When the substrate was glass, the refractive index of the dye-

#93332 - $15.00 USD Received 29 Feb 2008; revised 7 Apr 2008; accepted 15 Apr 2008; published 1 May 2008

doped polymer film was lower than that of the substrate, and a leaky waveguide or quasi-waveguide was obtained, where light is no longer fully confined: no total internal reflection takes place at the polymer film – glass substrate interface and light leaks into the substrate [41-46]. It has been pointed out that this feature could be a useful output coupling mechanism in an active-waveguide laser device [44-46], and a technique for measuring refractive indices and thicknesses of thin films based on leaky waveguides has been reported [42]. Our results seem to indicate a stronger self-mode-restriction capability in the quasi-waveguides as compared to the conventional total internal reflection waveguides.

## 2. Experimental

Planar waveguides consisting of dye-doped polymer films deposited onto quartz and glass substrates (0.88 mm and 0.98 mm thick, respectively) were produced by two different procedures: spin coating and extender roller. PMMA of 25,000 molecular weight (Polysciences, Inc.) in proportion 200 mg/mL was added to a solution of Toluene (Merck) containing PM567 (laser grade, from Exciton) at a concentration (with respect to polymer) of $5 \times 10^{-2}$ M. Although the dye concentration was rather high, photophysical studies did not show any evidence of aggregation of the dye molecules. Films with thickness around 5 μm and 17 μm were produced depending on the technique used. The thicker films were obtained by using the extender roller technique [47]. In this case, a few drops of the solution were placed on a standard glass microscope slide or quartz slide and extended along the slide with a calibrated rod (endless screw with calibrated thread). After solvent evaporation at room temperature, polymeric films of 17± 2 μm of thickness were obtained. Films with thickness of 5.5 ± 0.5 μm were obtained by spin coating (2000 rpm, 10s + 4000 rpm, 1s + 6000 rpm, 1s). In all cases, the thickness of the films was determined by using a gravimetric method (accuracy of balance, $10^{-4}$ g), taking into account the density of the polymeric film (1.19 g/mL).

The resulting quartz/glass – doped polymer – air structure defines an asymmetric slab optical waveguide. In the quartz-doped polymer-air structure, the measured refractive index of the dye-doped polymer layer ($n_1$ = 1.4900) is higher than the measured index of the quartz substrate ($n_2$ = 1.4583). Thus, total internal reflection at the film-quartz interface confines and guides the light along the film, and emission from the edge of the film is obtained. When the substrate is glass (measured index, $n_2$ = 1.5176), with higher refractive index than the doped polymer film, no total internal reflection takes place at the film-substrate interface and emitted light leaks into the substrate. A leaky waveguide or quasi-waveguide is obtained, where light is confined by the film-air interface while the reflection at the film-substrate boundary is leaky.

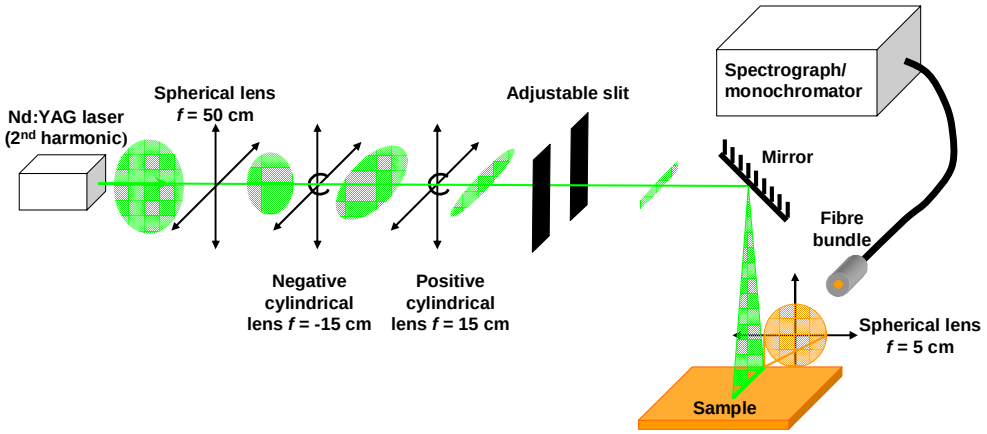


Fig. 1. Schematic of the experimental setup

#93332 - $15.00 USD Received 29 Feb 2008; revised 7 Apr 2008; accepted 15 Apr 2008; published 1 May 2008

The waveguides were optically pumped at 532 nm with 6 ns full width at half maximum (FWHM) pulses from a frequency-doubled *Q*-switched Ng:YAG laser (Monocrom OPL-10). The laser was typically operated at 1 Hz repetition rate, and the pulse energy was controlled by insertion of calibrated neutral density filters into the beam path. Pump energy was measured with a calibrated pyroelectric energy meter (ED200, GenTec). A schematic of the experimental setup is shown in Fig. 1. A combination of one spherical ($f$ = 50 cm) and two cylindrical quartz lenses ($f$ = −15 cm and +15 cm, respectively) perpendicularly arranged focused the pump beam to a narrow horizontal line onto the surface of the film. An adjustable slit was used to select only the central portion of the pump beam. The incident light was perpendicular to the substrate surface, and the excitation stripe on the sample was ~150 μm × 3 mm, with one end placed right up to the edge of the film. The edge emission from the sample was collected with a 5-cm focal length spherical lens, focused onto a fibre bundle and detected with a spectrograph/monochromator (SpectraPro-300i, Acton Research) equipped with a thermoelectrically cooled CCD detector (SpectruMM:GS 128B). A shortwave cutoff filter (OptoSigma, cutoff at 540 nm), placed before the fibre bundle avoids any scattered 532 nm light entering the spectrograph. At excitation intensities above a certain threshold value, the spontaneously emitted photons are amplified by stimulated emission as they travel along the stripe-shaped gain region and amplified spontaneous emission (ASE) occurs.

The net gain of the doped polymer film was measured by using the variable stripe length (VSL) method [48], which consists basically in pumping optically the sample with a stripe of variable length and measuring the intensity of the edge-emitted ASE as a function of stripe length. The stripe length was controlled by varying the width of the adjustable slit by means of a micrometer.

In an unsaturated amplifier having a length much greater than the diameter, the growth of intensity is governed by [49]:

$$\frac{dI(\lambda, z)}{dz} = g'(\lambda)I(\lambda, z) - \alpha I(\lambda, z) + \eta g'(\lambda), \tag{1}$$

where $g$' is the gain coefficient and $\alpha$ is the loss coefficient. The second term on the right side of (1) represents distributed losses, and the third term is the spontaneous emission, which has the same frequency dependence $g'(\lambda)$ as the gain coefficient. The coefficient $\eta$ is then proportional to the spontaneous emission rate and to a geometrical factor that depends on the amplifier dimensions. In the recent literature on waveguides, spontaneous emission proportional to pump intensity is usually described by a term $A(\lambda)P_0$ [3], and Eq. (1) is written with the substitution $\eta g'(\lambda) = A(\lambda)P_0$.

Integration of Eq. (1) with no input intensity ($I(\lambda,0) = 0$) leads to:

$$I(\lambda) = \frac{\eta g'(\lambda)}{g(\lambda)}(e^{g(\lambda)l} - 1), \tag{2}$$

where $g(\lambda)$ is the net gain coefficient, $g(\lambda) = g'(\lambda) - \alpha$, and $l$ is the length of the pumped stripe.

Eq. (2) represents the output intensity from one end of the stripe in the small-signal regime. Thus, in the absence of saturation, $g$ can be determined by plotting the intensity of the ASE emission as a function of the pumped stripe length and fitting the resulting curve to the expected dependence given by Eq. (2).

If the ASE intensity reaches the saturation level, Eq. (1) is no longer appropriate. This Eq. implies that the excited state population is always the same regardless of the ASE intensity. In order to take saturation effects into account, a term has to be included which accounts for the depletion of the excitation density. Consequently, Eq.(1) has to be replaced by [49]:

$$\frac{dI(\lambda, z)}{dz} = \frac{g'(\lambda)I(\lambda, z)}{1 + s\, I(\lambda, z)} - \alpha I(\lambda, z) + \eta g'(\lambda), \tag{3}$$

#93332 - $15.00 USD Received 29 Feb 2008; revised 7 Apr 2008; accepted 15 Apr 2008; published 1 May 2008

where $s$ is a saturation parameter ($s = 1/I_{sat} = \sigma\tau/h\upsilon$, where $\sigma$ is the emission cross section, $\tau$ is the fluorescence lifetime, and $\upsilon$ is the frequency of the ASE emission). Integration of this Eq. gives the behaviour of $I(\lambda)$ in both the small-signal and gain saturation regime.

The waveguide losses were characterized by measuring the optical loss coefficient by performing experiments where the stripe was gradually translated away from the edge of the sample while keeping the pumped stripe length constant ($l$ = 3mm). Assuming that the ASE emission from the end of the excitation stripe $I_0$ is constant, the emission from the edge of the sample should decrease as the stripe is displaced as a result of waveguide losses (absorption and scattering) following the Beer-Lambert law:

$$I = I_0 e^{-\alpha x}, \tag{4}$$

where $x$ is the length of the unpumped region between the end of the pump stripe and the edge of the sample. The loss measurements were performed by mounting the sample on a micrometric stage.

All the measurements were carried out at least three times at each pump intensity and an average value obtained. When quoted, the error is the standard deviation from the mean.

Table 1. Characteristics of the thin films studied and estimated threshold pump intensity ($I_{th}$) for ASE emission.

| Sample | Composition/solvent of initial solution | Method of preparation | Substrate | Thickness (μm) | $I_{th}$ (MW/cm$^2$) |
|---|---|---|---|---|---|
| **1** | PMMA(200 mg/mL) + PM567/toluene | Extender roller | Quartz | 15 | 1.85 |
| **2** | PMMA(200 mg/mL) + PM567/toluene | Spin coating | Quartz | 5 | 1.3 |
| **3** | PMMA(200 mg/mL) + PM567/toluene | Extender roller | Glass | 19 | 2.0 |
| **4** | PMMA(200 mg/mL) + PM567/toluene | Spin coating | Glass | 6 | 1.0 |

## 3. Results and discussion

### *3.1 Wave-guided ASE emission*

PM567 doped PMMA films deposited onto quartz substrates with the composition and thickness indicated in Table 1 (samples 1 and 2) were first prepared and studied.

Figure 2 shows the dependence of the full width at half maximum (open squares) and the intensity (filled squares) of the light emitted from the edge of the film with the pump intensity for sample 1. Pump intensity was varied from 0.21 MW/cm$^2$ up to 7.9 MW/cm$^2$. It can be estimated that at the lowest pump intensity 17% of the ground state population is excited whereas at the highest pump intensity the excited population was 88%. Fig. 3 shows the actual evolution of the emission spectra collected at various pump intensities for sample 2. Spectral narrowing of the spectra and a distinct change in the slope of the output emission intensity are observed with increasing pump intensity. The collapse of the FWHM in the emission spectrum and the change in the slope in the emission intensity are a signature of the onset of amplified spontaneous emission (ASE) above a certain pump threshold. Below threshold, the emission spectrum consists of a broad band characteristic of spontaneous emission which collapses to a FWHM of about 12 nm at pump intensities above threshold. The edge-emitted ASE showed a divergence of ~ 30 mrad in sample **1**, and of ~ 13 mrad in sample 2.

#93332 - $15.00 USD Received 29 Feb 2008; revised 7 Apr 2008; accepted 15 Apr 2008; published 1 May 2008

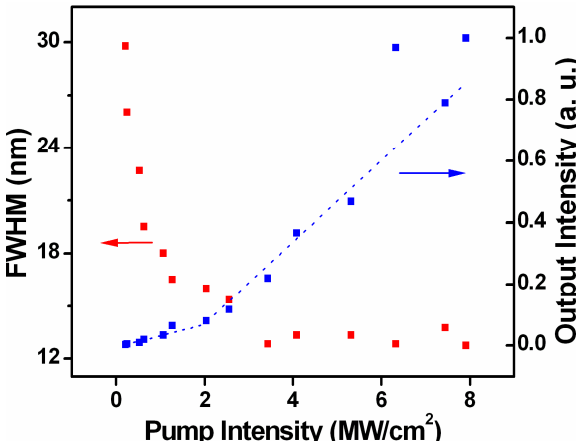


Fig. 2. Dependence of the FWHM of the emission spectra (open squares) and intensity of the output emission (full squares) on pump intensity for sample **1**. The dotted lines are a guide to the eye.

From the data in Fig. 2, a pump threshold for ASE emission of about 50 μJ (corresponding to a pump intensity of about 1.85 MW/cm$^2$) can be estimated for sample **1**. Up to this pump energy, the emission intensity increases slowly with pump intensity. Above threshold, the emission intensity increases sharply with pump intensity, and the FWHM of the emission levels off to values typical of ASE.

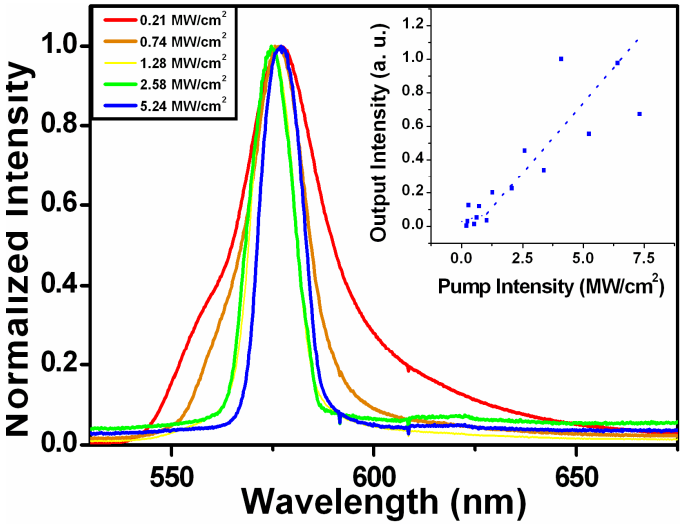


Fig. 3**.** Normalized emission spectra of sample **2** at different pump intensities. The inset represents the intensity of the output emission as a function of pump intensity. The dotted lines in the inset are a guide to the eye

Figure 4 shows the output intensity at the peak of the emission spectrum as a function of pump stripe length for sample **1**. Each point is an average of three measurements. The dashed line in Fig. 4 is a fit of the data to Eq. (2), which yields a net gain of 18.5 ± 4.1 cm$^{-1}$ at a pump intensity of 3.4 MW/cm$^2$. In Fig. 5, the output intensity of the ASE emission from sample **1** is plotted as a function of the distance of a 3 mm-length pump stripe to the edge of the sample, at a pump intensity of 3.4 MW/cm$^2$. Fitting the experimental data to Eq. (4) yields a loss coefficient of $\alpha = 3.8 \pm 0.4$ cm$^{-1}$. The first two points in the plot, corresponding to distances to

#93332 - $15.00 USD Received 29 Feb 2008; revised 7 Apr 2008; accepted 15 Apr 2008; published 1 May 2008

the edge of the sample shorter than half millimetre, do not fit in the exponential behaviour predicted by Eq. (4). Probably, some irregularity in the film near the edge precludes an effective pumping of this region.

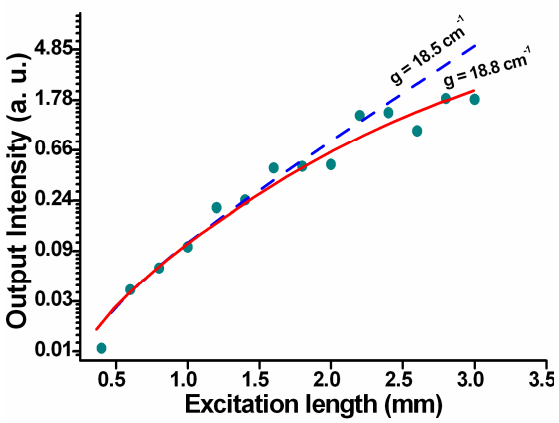


Fig. 4. Dependence of the emission intensity on excitation length for sample **1** at pump intensity of 3.4 MW/cm$^2$. The dashed line is a fit to the data using Eq.(2). The solid line is a fit to the data using Eq.(6).

The results obtained with sample 2 exhibit more scattering than those obtained with sample 1 (see inset in Fig. 3), probably due to the smaller thickness of sample **2**. At a PM567 concentration $5\times10^{-2}$ M, a sample 15 μm thick absorbs about 82% of the incoming pump radiation at 532 nm, whereas a sample 5 μm thick only absorbs 44% of the pump radiation, being thus more sensitive to pump conditions and fluctuations. Threshold for ASE emission is at a pump intensity of about 1.3 MW/cm$^2$. By fitting Eq. (2) to the experimental data of output intensity as a function of pump stripe length (Fig. 6, dashed line), a net gain of $15.7 \pm 4.6$ cm$^{-1}$ is estimated at 3.4 MW/cm$^2$ pump intensity. Fig. 7 shows the variation of the output intensity when the pump stripe was gradually translated away from the edge of the sample when the pump intensity was 3.4 MW/cm$^2$. The solid line is a fitting of the data to Eq. (4), yielding a loss coefficient of $6.1 \pm 1.3$ cm$^{-1}$.

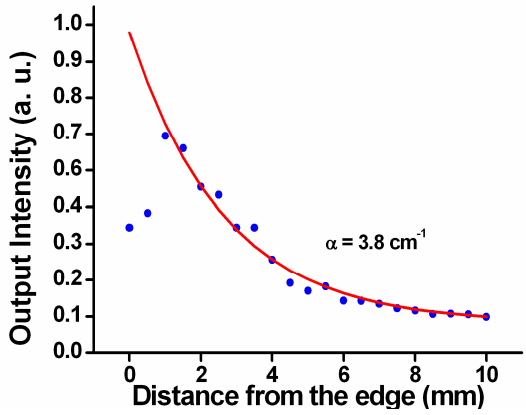


Fig. 5. Intensity of the light emitted from the edge of the waveguide as a function of the distance between the pump stripe and the edge of the sample for sample **1** at 3.4 MW/cm$^2$ pump intensity. The solid line is a fit to the data using Eq.(4).

#93332 - $15.00 USD Received 29 Feb 2008; revised 7 Apr 2008; accepted 15 Apr 2008; published 1 May 2008

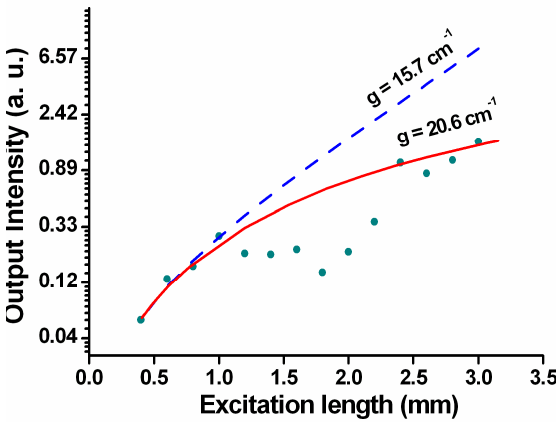


Fig. 6. Dependence of the emission intensity on excitation length for sample **2** at pump intensity of 3.4 MW/cm$^2$. The dashed line is a fit to the data using Eq.(2). The solid line is a fit to the data using Eq.(6).

*3.2 Leaky-mode emission*

Next, ASE emission from quasi-waveguides, where the gain medium was deposited onto a substrate with higher value of the refractive index, was studied. At the doped-polymer – air interface, light propagating at angles greater than the critical angle $\theta_c$ = 42 º will be totally reflected, while at the doped-polymer – glass interface no total reflection takes place at any angle, and light leaks into the substrate. Nevertheless, even in this case, where the refractive index of the film is smaller than the substrate refractive index, the large reflectivity occurring at grazing incidence leads to significant confinement of the light [42]. The different transverse modes propagating within the gain layer have different reflectivity losses due to the Fresnel law. The fundamental mode is the one with lower losses and, thus, light is amplified preferably in this mode, which means that in a quasi-waveguide there is much stronger self-mode-restriction capability than in a conventional total internal-reflection waveguide. However, when the thickness of the gain layer is large compared with the wavelength of the light, several low-loss leaky modes may exist [41].

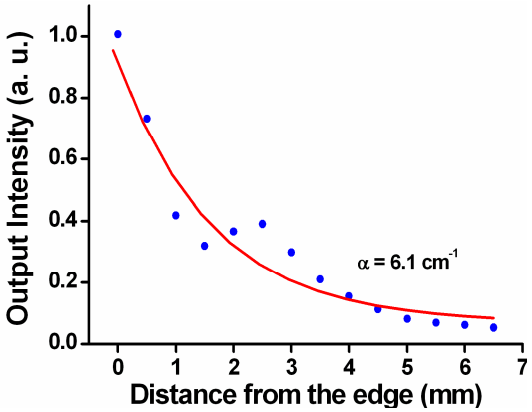


Fig. 7. Intensity of the light emitted from the edge of the waveguide as a function of the distance between the pump stripe and the edge of the sample for sample **2** at 3.4 MW/cm$^2$ pump intensity. The solid line is a fit to the data using Eq.(4).

Divergence of the edge-emitted ASE was ~ 100 mrad for both samples **3** and **4**. The fact that the ASE divergence is the same in both samples, independently of their thickness,

#93332 - $15.00 USD Received 29 Feb 2008; revised 7 Apr 2008; accepted 15 Apr 2008; published 1 May 2008

whereas in the waveguides (samples 1 and 2) the divergence of the light emitted by the thinner waveguide is lower than that of the light emitted by the thicker one is a confirmation of the quasi-waveguiding character of the light emitted when the films were deposited onto glass substrate, as it has been shown that in the emission from conventional waveguides there is a strong dependence of the properties of the emitted light on the thickness of the film [50].

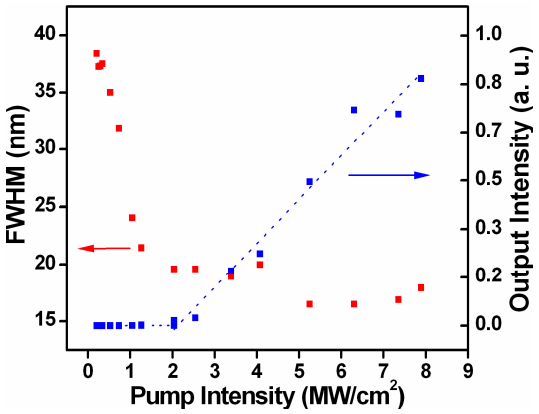


Fig. 8. Dependence of the FWHM of the emission spectra (open squares) and intensity of the output emission (full squares) on pump intensity for sample **3**. The dotted lines are a guide to the eye.

Figures 8 and 9 show the dependence of the FWHM of the emission spectra and intensity of the output emission on pump intensity for samples 3 and 4, respectively. Threshold pump intensities for the onset of ASE emission are clearly discernable in those plots and are found to be about 2.0 MW/cm$^2$ and 1.0 MW/cm$^2$, respectively. In this case reducing the film thickness results in a significant decrease in ASE threshold, whereas in the waveguides over quartz substrate this decrease is not so important.

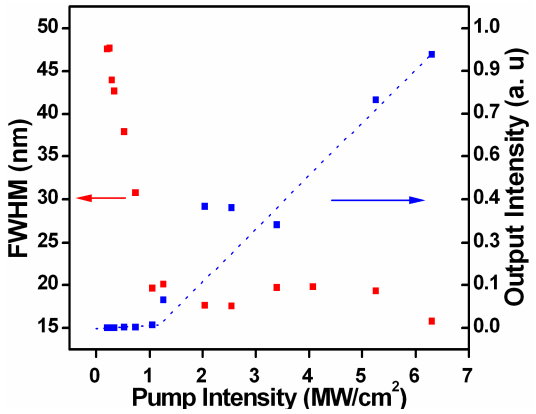


Fig. 9. Dependence of the FWHM of the emission spectra (open squares) and intensity of the output emission (full squares) on pump intensity for sample **4**. The dotted lines are a guide to the eye.

In Fig. 10 and 11, the emitted light intensity for samples 3 and 4 is plotted as a function of excitation length for different pump intensities. In the derivation of Eq. (2) gain saturation was not considered; thus, when using this Eq. to estimate the net gain coefficients only those subsets of data for which gain saturation is not evident should be used in the fitting procedure. The dashed lines in Fig. 10 and 11 are the fitting of the data using Eq. (2), leading to the net gain values collected in Table 2. Gain saturation, which is clearly evident in some of the plots

#93332 - $15.00 USD Received 29 Feb 2008; revised 7 Apr 2008; accepted 15 Apr 2008; published 1 May 2008

in those Fig., occurs because the light travelling in the sample is so strongly amplified that it depleted a substantial fraction of the excitation. As gain saturation sets in, the gain coefficient is reduced and light is no exponentially amplified further as the length of the pumped stripe is increased. Sample degradation can be ruled out as the cause of saturation seen in Fig. 10 and 11 because each point was obtained by pumping a fresh region. From close inspection of both Fig., it can be appreciated that gain saturation onsets at $gl \approx 4$. This is not surprising since spontaneous emission that is amplified by a factor exp(4) is most likely intense enough to significantly depopulate the excitation density, as has been pointed out by McGehee *et al.*[48].

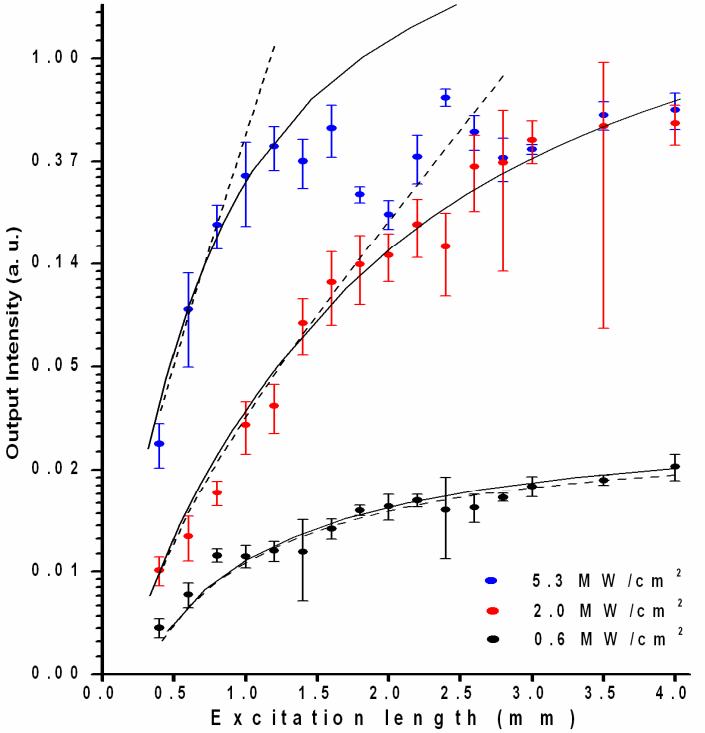


Fig. 10. Dependence of the emission intensity on excitation length at various pump intensities for sample **3**. The dashed lines are fits to the data using Eq.(2). The solid lines are fits to the data using Eq. (6).

As saturation effects are important except at the lower pump energies in these plots, using Eq. (2), even restricted to the subsets of data apparently free of saturation effects, could lead to appreciable errors in the calculated gain coefficients. Thus, to obtain a better estimation of the gain coefficients Eq.(3), which includes saturation effects, should be used as starting point.

In our experimental conditions, and supposing loss coefficients of the order of those obtained in the waveguide studies reported in the previous section, the product $\alpha s I$ is small compared to the gain coefficient $g(\lambda)$. Thus, we can replace Eq. (3) with the approximate expression:

$$\frac{dI(\lambda,z)}{dz} = \frac{\eta g'(\lambda) + [\eta g'(\lambda) s + g(\lambda)] I(\lambda,z)}{1 + s\, I(\lambda,z)}, \tag{5}$$

which, integrated between 0 and $I_t(\lambda)$ (total intensity) and between 0 and $l$, leads to:

$$l = s\, I_t(\lambda) + \frac{1 - \eta g'(\lambda) s}{g(\lambda) + \eta g'(\lambda)} \ln \left| \frac{\eta g'(\lambda) + [\eta g'(\lambda) + g(\lambda)] I_t(\lambda)}{\eta g'(\lambda)} \right|, \tag{6}$$

#93332 - $15.00 USD Received 29 Feb 2008; revised 7 Apr 2008; accepted 15 Apr 2008; published 1 May 2008

which can be used to fit the data in Fig. 10 and 11. Thus, $g$ can be determined by plotting the pumped stripe length as a function of the intensity of the ASE emission and fitting the resulting curve to the expected dependence given by Eq. (6). As this Eq. depends on three parameters, the fit is very sensitive to the initialization values. In order to get a univocal fitting, it is convenient to use the value of $\eta g$' calculated with Eq. (2) as a fixed parameter, since it should not be affected by saturation.

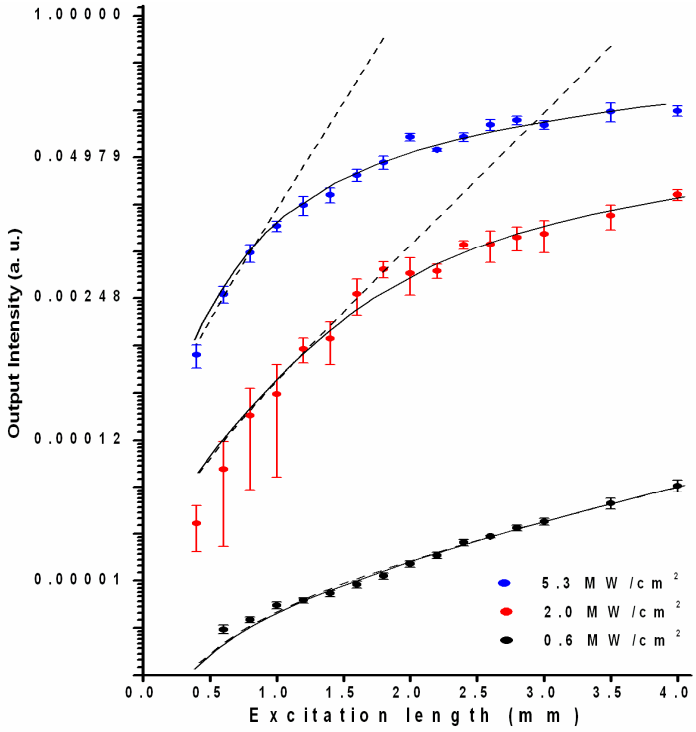


Fig. 11. Dependence of the emission intensity on excitation length at various pump intensities for sample **4**. The dashed lines are fits to the data using Eq.(2). The solid lines are fits to the data using Eq. (6).

Table 2. Net gain coefficients $g$ at different pump intensities $I_p$ for waveguides and quasi-waveguides obtained by using Eq. (2) (upper values) and Eq. (6) (lower values, in italic)

| $I_p$ | $g$ (cm$^{-1}$) | | | |
|---|---|---|---|---|
| (MW/cm$^2$) | Sample **1** | Sample **2** | Sample **3** | Sample **4** |
| 5.3 | | | 42.4±5.4 | 45.1±4.3 |
| | | | *51.7± 8.4* | *56*± 9 |
| 3.4 | 18.5±4.1 | 15.7±4.6 | | |
| | *18.8*± 2.0 | *20.6*± 0.7 | | |
| 2.0 | | | 17.4±2.4 | 28.1±1.7 |
| | | | *20.1± 2.5* | *29.9± 1.9* |
| 0.6 | | | –4.2±0.7 | 6.7±0.2 |
| | | | *–4.1± 0.1* | *6.9± 0.9* |

#93332 - $15.00 USD Received 29 Feb 2008; revised 7 Apr 2008; accepted 15 Apr 2008; published 1 May 2008

The solid lines in Fig. 10 and 11 are the fitting of the data using Eq. (6).Using the same Eq. with the data of the waveguides, the solid lines in Fig. 4 and 6 are obtained. In Table 2 are collected the net gain coefficients $g$ at different pump intensities $I_p$ for both waveguides and quasi-waveguides, obtained by using both Eq. (2) and (6). The numbers in italics are the net gain coefficients estimated by using the more complete Eq. (6). It is seen that when saturation effects results are taken into account the net gain coefficients obtained are higher than those estimated using the small-gain expression. As expected, the differences in the values between the two sets of net gain coefficients are more important at high pump intensities, where saturation sets in earlier.

To put our results in perspective is useful to compare the net gain values obtained in this study with previous gain measurements performed on dye doped polymer films. Some authors use fluence (mJ/cm$^2$) instead of intensity (W/cm$^2$) to characterize the incident pump radiation. In our case, the intensities in Table 2 correspond to fluences in the range 3.7 mJ/cm$^2$ (intensity of 0.63 MW/cm$^2$) to 32 mJ/cm$^2$ (intensity of 5.3 MW/cm$^2$).

With pumping at 532 nm, gains of up to 40 cm$^{-1}$ were obtained with optical waveguides based on polystyrene films doped with dye 4-(di-cyanomethylene)-2-*t*-butyl-6(1,1,7,7-tetramethyljulolidyl-9-enyl)-4*H*-pyran (DCJTB) and pumped with pulses of 0.13 mJ (Lu *et al*.[29]); the net gain increased to 52.71 cm$^{-1}$ when a mixture of dyes DCJTB and 10-(2-benzothiazolyl)-1,1,7,7-tetramethyl-2,3,6,7-tetrahydro-1*H*,5*H*,11*H*-[1] benzopyrano [6,7,8-*ij*]quinolizin-11-one (C545T) codoped in polystyrene films was used at a pump energy of 0.08 mJ/pulse (Zhang *et al*.[18]). In both cases no pump fluence nor intensity was given. Oton *et al*.[36], obtained net gain coefficients of 8.7 cm$^{-1}$ when pumping at fluences of 27.0 mJ/cm$^2$ with dye Nile blue (LC 6900) incorporated into oxidized porous silicon planar waveguides, and Calzado *et al*.[21] reported gain coefficients up to 10 cm$^{-1}$, at a pump intensity of 74 kW/cm$^2$ with perylenediimide derivatives in polystyrene films. Pumping with 100 mW of continuous radiation at 488 and 514 nm, Manaa *et al*.[4] obtained net laser gains of up to 53 cm$^{-1}$ in plastic slab doped with perylimide dyes. In the near infrared region, Casalboni *et al*.[38] estimated an optical gain of about 11 cm$^{-1}$ for polymethine dye IR1051 in hybrid sol-gel channel waveguides with a pump intensity of 300 W/cm$^2$ at 1064 nm.

With pumping at 355 nm, Kretsch *et al*.[3] obtained net optical gains of $g$ = 15-20 cm$^{-1}$ at pump intensity of 0.87 MW/cm$^2$ on stilbenoid and perylene vinylene derivative in polystyrene waveguides; Tsutsumi *et al*.[13] observed optical gain of up to 13.8 cm$^{-1}$ for 1,4-Bis[2-[4-[N,N-di(p-tolyl)amino]phenyl] vinyl]benzene (BTAPVB) dye incorporated into different polymers with pump fluences higher than 20 mJ/cm$^2$; Jordan *et al*.[25] reported gains of 84 cm$^{-1}$ on substituted stilbene-dye-doped polymer waveguide under pumping with pulses of 1.1 mJ/cm$^2$; Saraidarov *et al*.[39] obtained a gain factor of 14 cm$^{-1}$ for blue laser dye Direct White in sol-gel inorganic-organic hybrid films at a pump intensity of 5 MW/cm$^2$, and Pisignano *et al*.[26] found a maximum gain coefficient of 5.6 cm$^{-1}$ with photochromic molecule indolinospiropyran (1',3'-dihydro-1',3',3'-trimethyl-6-nitrospiro [2H-1-benzopyran-2,2'-(2H)-indole]) (6-nitro-BIPS) doped in polymer matrix at a pump fluence of 0.5 mJ/cm$^2$.

From the above comparison it is seen that the values of the net gains measured in this work compare well or are higher than those obtained in similar systems reported in the bibliography.

It is seen in Table 2 that whereas in the waveguides decreasing the film thickness results in a small variation in the gain, in the quasi-waveguides the net gain coefficient increases significantly when the thickness of the film is reduced from 19 to 6 μm. This could be understood in terms of the stronger self-mode-restriction capability in the quasi-waveguides. In the thicker quasi-waveguide (sample 3), more guided modes are allowed to propagate than in the thinner films. The higher-order modes have greater losses than the fundamental and lower-order ones, because light emitted in those modes leaks preferentially to the substrate and is no longer amplified. In the thinner quasi-waveguide (sample **4**), a lower number of modes are allowed and more pump energy appears as amplified light in the fundamental and low-loss lower-order leaky modes, which results in increased gain. In the waveguides (samples **1** and **2**), the modes are not leaky, there are no losses to the substrate, and in both

#93332 - $15.00 USD Received 29 Feb 2008; revised 7 Apr 2008; accepted 15 Apr 2008; published 1 May 2008

thick and thin films the light in all the allowed modes is amplified so that the gain is close in both cases. The same effect could explain the much higher decrease in the threshold for ASE emission observed in the quasi-waveguides as compared with the waveguides.

## 4. Summary and conclusions

We have studied the amplified spontaneous emission and gain characteristics of planar waveguides and quasi-waveguides consisting of PM567-doped PMMA films deposited onto quartz or glass substrates, respectively. Two different methods of preparation were tried: spin-coating and extender roller, leading to films with thicknesses of about 5 μm and 17 μm, respectively.

By following the evolution of the spectral FWHM and the intensity of the light emitted from the edge of the film with increasing the pump intensity, the threshold for ASE emission, characterized by the collapse of the FWHM in the emission spectrum and the change in the slope of the emission intensity, was determined and found to be lower in the thinner films. Threshold values were about 1.0 $MW/cm^2$ for the thinner films and about 2.0 $MW/cm^2$ for the thicker ones.

The study of the dependence of the intensity of the ASE emission with the length of the pump stripe at different pump intensities allowed estimating net gain coefficients by fitting the experimental points with appropriate theoretical expressions. The usual approach of considering a one-dimensional amplifier in the small-signal regime leads to an expression widely used to estimate optical gain in thin films, but that is only appropriate when saturation effects are not present. We show that a modification of the small-signal expression incorporating saturation effects allows obtaining an analytic solution in the intermediate saturation regime which leads to a better fitting of our experimental results. In this way, we estimated net gain coefficients of up to $56 \pm 9$ $cm^{-1}$ at a pump intensity of 5.3 $MW/cm^2$ for quasi-waveguides and up to $20.6 \pm 2.7$ $cm^{-1}$ at a pump intensity of 3.4 $MW/cm^2$ for waveguides. Loss coefficients in the waveguides were estimated to be $3.8 \pm 0.4$ $cm^{-1}$ and $6.1 \pm 1.3$ $cm^{-1}$ for the thicker and the thinner films, respectively.

The results obtained seem to indicate a stronger self-mode-restriction capability in the quasi-waveguides that in the waveguides based in the increased losses in the higher-order leaky modes in the quasi-waveguides, where the large reflectivity occurring at grazing incidence leads to significant confinement of the light in the lower-order modes.

## Acknowledgments

This work was supported by Projects MAT2004-04643-C03-01 and MAT2007-65778-C02-01 of the Spanish CICYT.

#93332 - $15.00 USD Received 29 Feb 2008; revised 7 Apr 2008; accepted 15 Apr 2008; published 1 May 2008